MICROFRACTOGRAPHY OF STATIC TENSILE TESTS FRACTURES OF 1.4539 AUSTENITIC STEEL AND 1.4742 FERRITIC STEEL WELDED JOINTS

Barbara NASIŁOWSKA[1], Zdzisław BOGDANOWICZ[2], Janusz FLĄDRO[3], Mariusz NOGA[4], Paweł PASTUSZKA[2], Bartosz SIERAKOWSKI[1], Kaziemierz ZEGAR[4]

[1] Military University of Technology, Institute of Optoelectronics, Poland, 00-908, Warsaw, Kaliskiego St., 2
[2]Military University of Technology, Faculty of Mechanical Engineering, Poland, 00-908, Warsaw, Kaliskiego St., 2
[3]Zakłady Budowy Aparatury Chemicznej – Grupa Azoty w Tarnowie, Poland, 33-101, Kwiatkowskiego st. 8, Tarnow
[4]Grupa Azoty PROREM Sp. z o.o., Poland, 47-220, Mostowa st. 24 D Kędzierzyn – Koźle

The paper presents the results of microfractography of static tensile test fractures of welded joints of 1.4539 austenitic steel and 1.4742 ferritic steel utilized for chemical installations production. The tested types of steel resistant to corrosion indicated two different types of fracturing. In case of ferritic steel, it was brittle fracturing on the boundaries of grains, whereas, in case of austenitic steel it was plastic fracturing.

INTRODUCTION

Fracture in plastic materials occurs when the material consistency is exceeded in the slip planes. In [3] metallurgical and mechanical properties of autogeneous and activated compound flux assisted gas tungsten arc welding (GTAW) of super-austenitic stainless steel, AISI 904L were compared. Compound flux containing 85% SiO2–15% TiO2 was used. Tensile studies showed that the fracture occurred at the fusion zone for both the weldments. Ductility was found to be greater for the flux-assisted weldments. This paper also investigates the structure–property relationships of AISI 904Lweldments using the combined techniques of optical and scanning electron microscopy.

Document [4] presents that the tensile test was carried out, and the yield strength and tensile strength of the joints were determined and their fracture surfaces were analyzed through scanning electron microscope (SEM). The tensile test was carried out, and the yield strength and tensile strength of the joints were determined and their fracture surfaces were analyzed through SEM. Finally, the FW parameters were optimized using PSO technique. It was found, that difficult weld by fusion welding process material can easily weld by FW process.

Paper [5] presents the bead geometry, microstructure and mechanical properties of AISI 904 L super austenitic stainless steel joint by CO2 laser-GMAW hybrid welding process. A detailed study of CO2 laser-GMAW hybrid welding with different shielding gas mixtures in different ratio (50%He+50%Ar, 50%He+45%Ar+5%O_2, and 45%He+45%Ar+10%N_2) was carried out on AISI 904 L super austenitic stainless steel sheet of 5 mm thickness. The X-ray diffraction was used to analyze the phase composition, while the microstructural characterization was performed by phase microscopy of the joints. The impact and tensile tests were performed and fracture surface morphology had been analyzed through scanning electron microscope (SEM). The results showed that the joint by laser-GMAW hybrid had higher tensile and impact strength than the base metal. The fractrography observation showed the cup-cone shaped fracture while the hybrid welding joint mixed mode of fracture.

Nanoindentation experiments were conducted by using a Triboindenter instrumented nanoindenter (Hysitron, USA), calibrated on pure aluminum and silica on the deformed stainless steel 904L and 316L what as described in [6]. Grain boundaries with twinning boundaries is higher than that without twinning boundaries for 904L SS, it should be the effect of twin boundaries

existence. The texture evolution of rolled 904L stainless steel which is austenitic phase were symmetrically at room temperature to different reductions, i.e., 0%, 20%, 40%, 60%and 80% were also researched, the result suggests a strong influence of the micromechanical incompatibility of the austenite phases on the texture evolution.

Characterization of intermetallic phases formed in the heat affected zone of a welded superaustenitic stainless steel of composition Fe–0·02C–3Mn–24Cr–7·3Mo–22No–0·5Cu–0·5N (wt %) was presented in [7]. Grain boundary precipitates at various distances from the fusion line have been investigated regarding crystal structures, compositions, and particle morphologies. A correlation of precipitation with the temperature history recorded in the heat affected zone was also performed. Two different precipitates, σ and R, were detected in the heat affected zone. These precipitates were evenly distributed along grain boundaries and had platelike shapes with typical lengths of 200–900 nm and 30–300 nm for σ and R, respectively. Near the fusion line, coexistence of R and σ phases was observed but, at larger distances, only R phase was found, indicating a lower temperature of formation for this phase. The available analysis of literature lacks a detailed comparative analysis of micrography of a static attempt to break welded joints of 1.4539 and 1.4742 stainless steel operating in the chemical installations.

The article purpose is to determine the properties of material, the crystallise structure as well as the purity and homogeneity based on the microfractography of static tensile test fractures of welded joints of 1.4539 austenitic steel and 1.4742 ferritic steel.

1. RESEARCH OBJECT

Welded joints made of 1.4539 austenitic steel with TIG method and made of 1.4742 ferritic steel with MAG method were subjected to comparative investigations of a static tensile test.

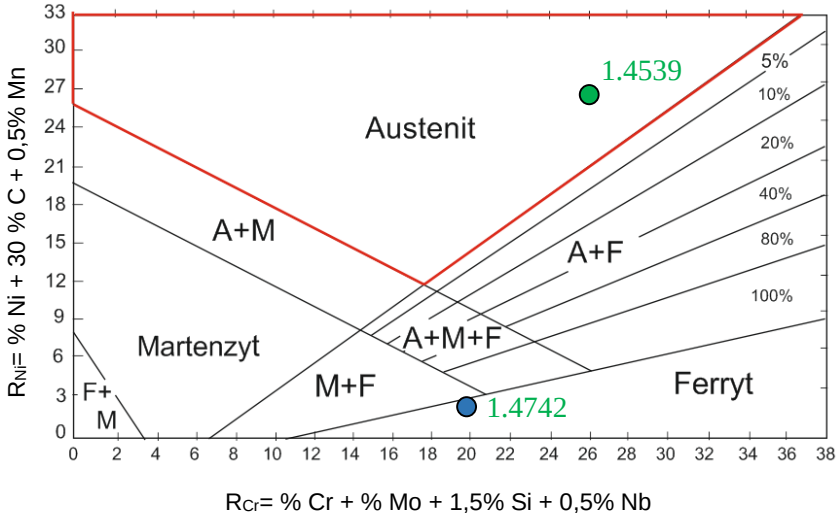

Fig. 1. Shaeffler's chart, for determining the phase components, with an equivalent chemical composition of the tested 316L steel marked [8]

According to L. A. Schaffler, a weld structure after it is completely cooled down depends on the ratio of austenite-forming components to ferrite-forming components [8, 9]. The considered types of corrosion resistant steels differ with a content of austenite-forming and ferrite-forming components responsible for forming the area of ferrite (Fig. 1). Chemical composition of the analyzed samples as delivered is presented in Table 1.

Table 1. Chemical composition of 1.4539 and 1.4742 steels

zaw. proc percentage	C	Si	Mn	P	S	Cr	Mo	Ni	Inne other
1.4539	≤0.02	≤0.70	≤2.00	0.030	≤0.010	19.0÷21.0	4.0÷5.0	24.0÷26.0	N≤0.15 Cu 1.20÷2.00
1.4742	>0.12	0.70÷1.40	>1.00	>0.04	>0.015	17.0÷19.0	-	-	Al: 0.70 ÷1.70

TIG and MAG welds were made according to the same production technology as is utilized in Zakłady Budowy Aparatury Chemicznej – Grupa Azoty in Tarnow. After chamfering edge (V)

(Fig. 2a), there was conducted a welding process through two passages from the face side (Fig. 2 c – *1* and *2*), then the weld ridge was undercut (Fig. 2 b – grinding) and pre-welded (Fig. 2 c – 3).

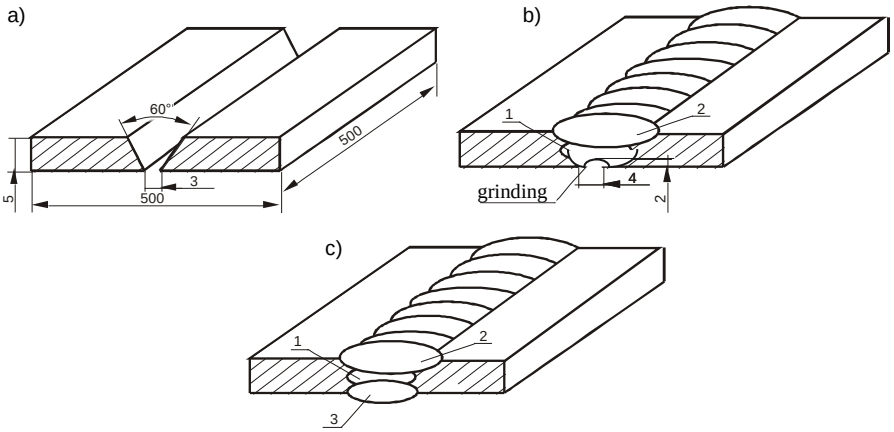

Fig. 2. Geometry of metal sheet elements preparation before welding (a) and a scheme of weld ridge undercutting (b) and pre-welding (c) according to technology utilized in Zakłady Budowy Aparatury Chemicznej – Grupa Azoty in Tarnow

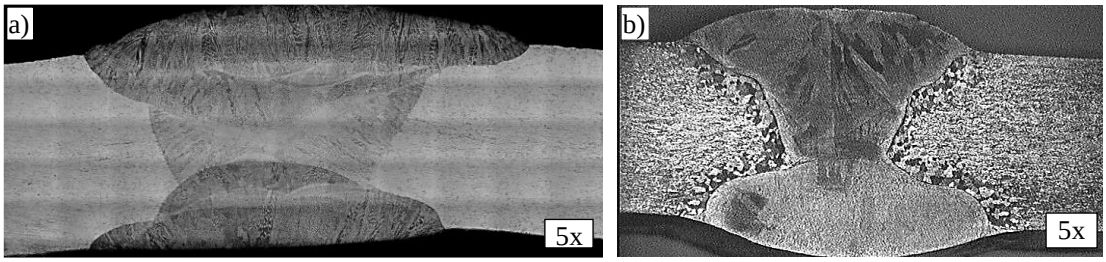

Fig. 3. Structure of a weld made of 1.4539 austenitic steel with TIG method and weld made of 1.4742 ferritic steel with MAG method

Structural analysis of metallographic microsections (Fig. 3) proved that a flat coagulation front with a gradual fusion of grain boundaries occurred in the weld made with TIG method. A clearer growth of the grains near the fusion line in the heat affected zone occurred in the welded joint made of 1.4742 ferritic steel compared to the joint made of 1.4539 austenitic steel. In the heat-affected zone, where the material did not undergo fusion, fast fluctuations in temperature caused structural changes characterized with coarseness.

The material of the weld, which underwent a total fusion during welding, after transition into the solid state, was characterized with a dendritic structure in the pillar form perpendicularly oriented to the heat dissipation front.

Based on the tests results, mechanical properties of 1.4539 austenitic steel and 1.4742 ferritic steel were determined in respect to normative values.

Table 2. Mechanical properties of 1.4539 and 1.4742 steels

	R_m [MPa]
1	*2*
1.4539 austenitic steel with TIG weld	589
1.4539 austenitic steel according to PN-EN 10027-1 standard	530-570
1.4742 ferritic steel with MAG weld	547
1.4742 ferritic steel according to PN-EN 10095 standard	500 - 700

2. TEST CONDITIONS

Mechanical properties of flat samples with a weld, with dimensions given in Fig. 4, made with TIG method were determined in accordance with PN-EN ISO 6892-1:2010 standard.

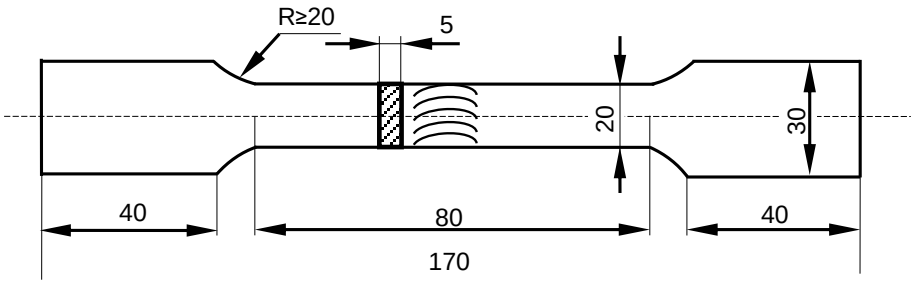

Fig. 4. Dimensions of 1.4539 austenitic steel sample with a weld for mechanical properties research

3. RESEARCH RESULTS

Distributive fractures in the static tensile test of the considered 1.4539 steel welded joints occurred in the base material zone outside the weld. A noticeable necking creating a so-called neck with curved side outlines of the fracture with a visible stratification generated after rolling is typical for flat samples made of plastic materials.

The biggest delamination of the material observed on the fracture occurs in the middle of the fracture, which results from stress distribution in the neck and its surrounding. The greatest tensile stress resulting from necking occurs in the middle of the fracture. The beginning of the fracture (fracturing initiation) should be, thus, expected in the sample axis or in its surrounding (Fig. 5). With intensification of necking there occurred shear of the material layers in direction of the most convenient slips until a distributive fracture was generated. Local shears of material also prove material ability to considerable plastic strain in the analyzed welded joints (Fig. 6 c, d).

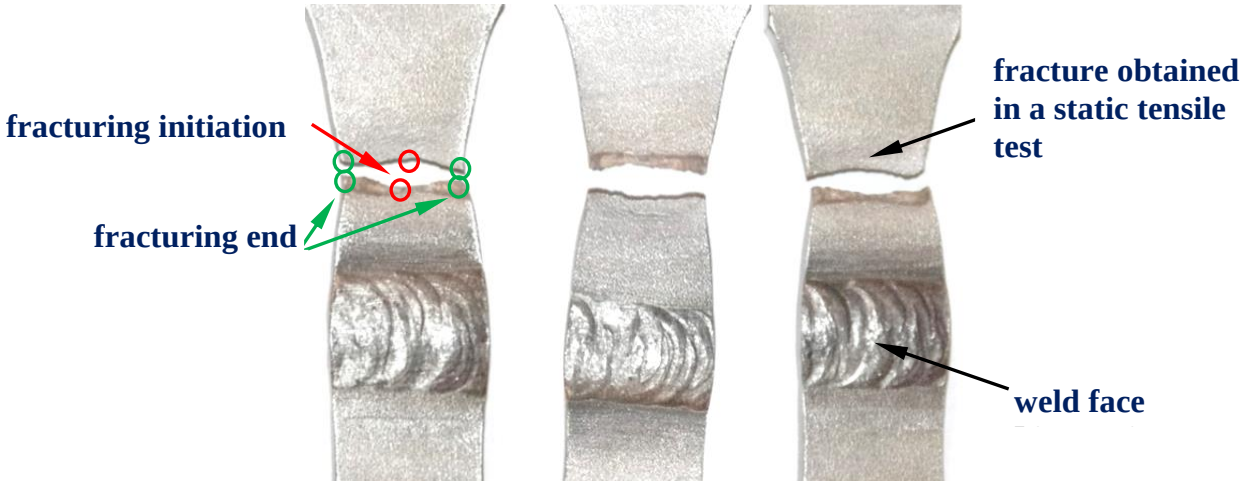

Fig. 5. Fracture obtained in a static tensile test of 1.4539 steel welded joint made with TIG method

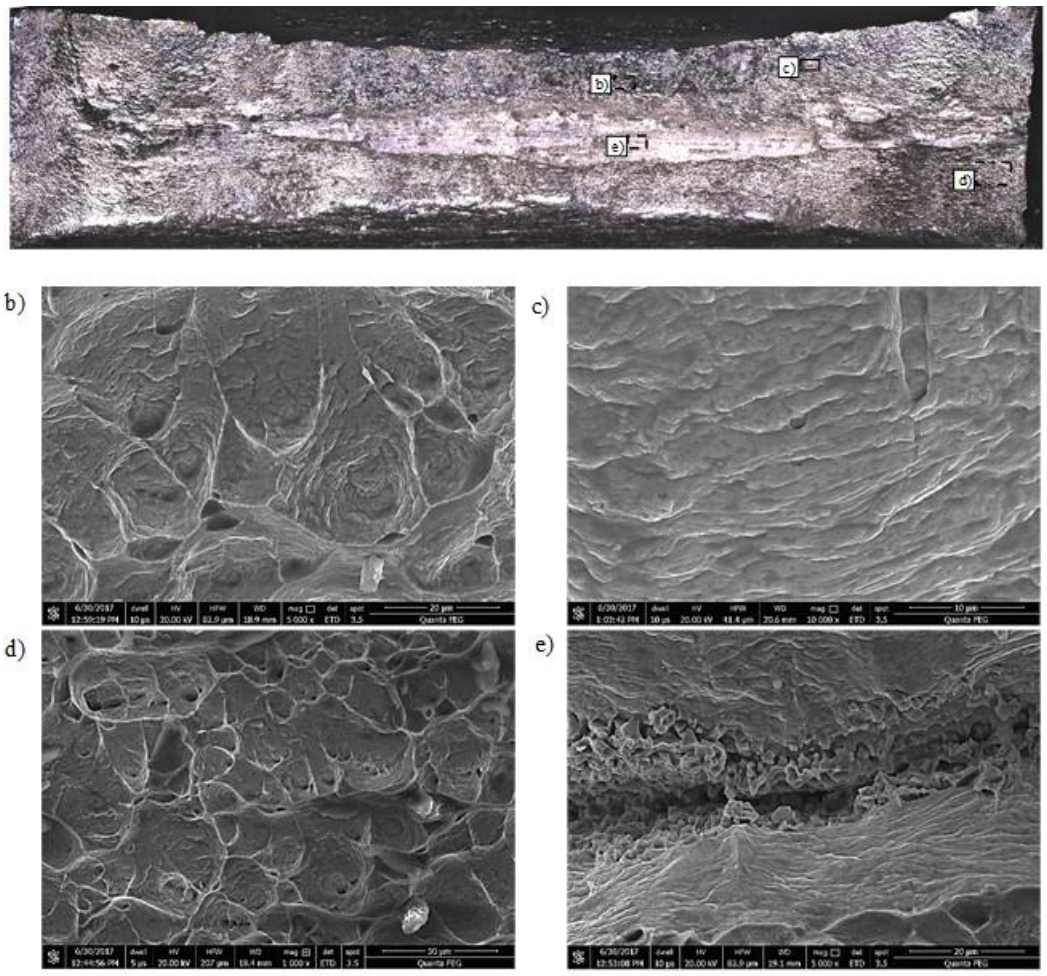

Fig. 6. Microstructure of flat sample fracture of 1.4539 austenitic steel welded joint obtained in a static tensile test

Fig. 6e shows delamination of the material, with a visible texture resulted from hot rolling of the metal sheets, in the central axis of the sample parallel to the rolling plane (Fig. 6 e). The fractures were characterized by systems of cavities and protrusions creating a kind of plastic structure typical for plastic fracturing (Fig. 6 a, b, c, d). The intrusions occurred during loading and resulted from impurity of the material after rolling (Fig. 6 b, c, d). They enlarge due to plastic strain and plastic decohesion.

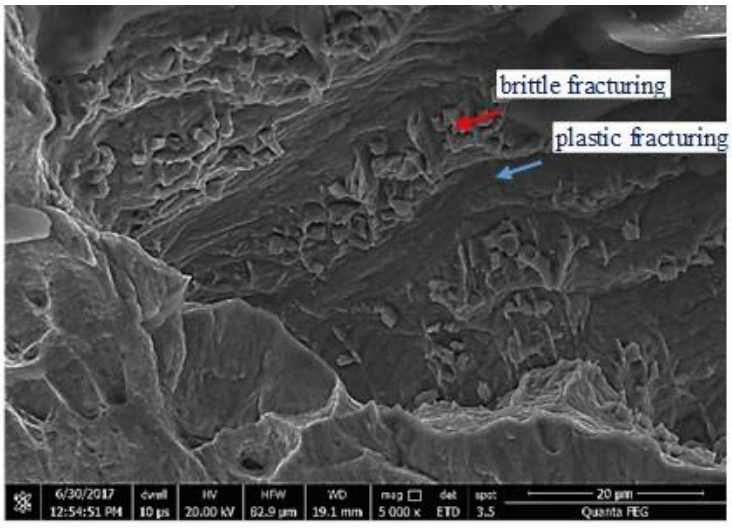

Fig. 7. Local mixed fracturing of 1.4539 austenitic steel

In the outer areas of the fracture, there was observed mixed fracturing, i.e., sections of brittle and plastic scrap occurring alternately (Fig. 7).

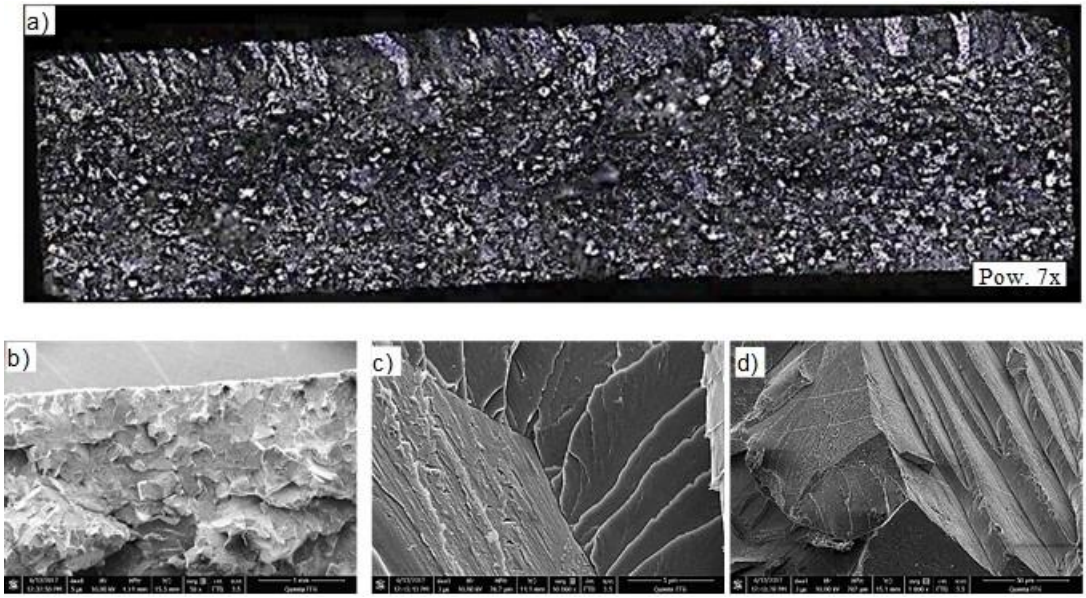

Fig. 8. Structure of ferritic steel weld made with MAG method

A static fracture of 1.4742 ferritic steel joints welded with MAG method was characterized with brittle fracturing (Fig. 8 a) without clear signs of necking and was perpendicular to sample tensile axis. There were observed numerous fissile fractures (Fig. 8 c, d, Fig. 9 b, c), intercrystallite fractures (Fig. 8 b) and fractures on the grains boundaries (Fig. 9 a). Fractures on the grains boundaries result from lower material coherence, when the surface energy of the grains boundaries is lower than the energy in cleavage planes [11].

Fracturing occurred mainly in the planes typical for chromium (110), (112), (11) and iron (100). There were also observed fractures in the cleavage planes (Fig. 9 c) and secondary fractures (Fig. 9 d). Figure 8 presents separation of the grain from the material structure. A clear outline of the grain boundaries proves a considerable harder structure of the inclusion which, due to an influence of ultimate strength on the sample, was separated in whole.

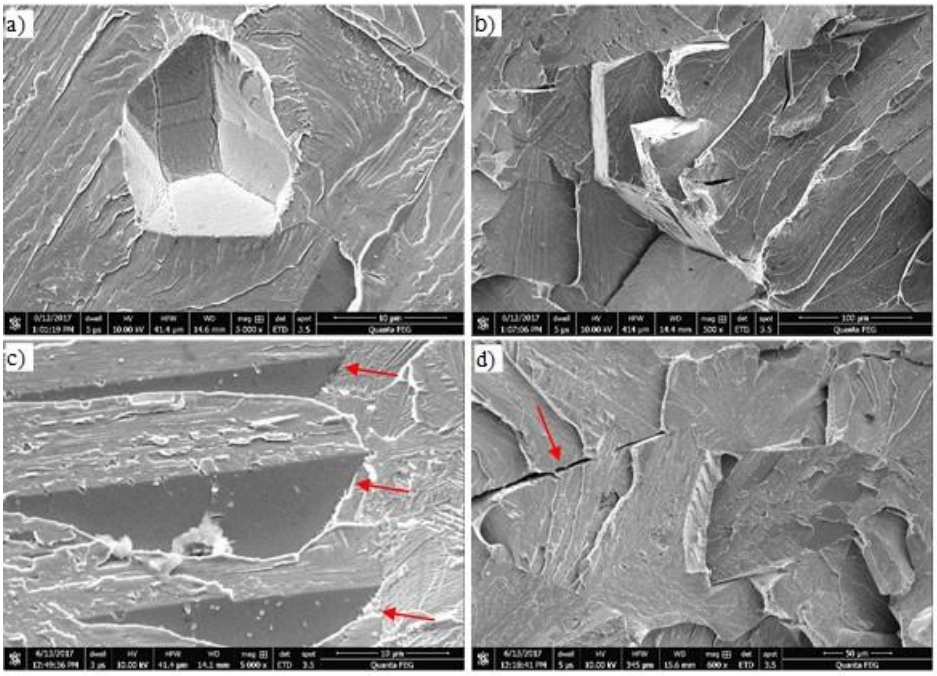

Fig. 9. Surface of brittle fracture on 1.4742 ferritic steel grain boundary

In the final stage of fracturing, in the grains boundaries zone, there was observed plastic and brittle fracturing. Primary brittle fracturing occurred along transcrystalline planes and grains boundaries, and then local slips occurred on the tops and edges of the grains (Fig. 10). There were observed minor numerous nucleating pins on the grains boundaries (indicated by blue arrows, Fig 10).

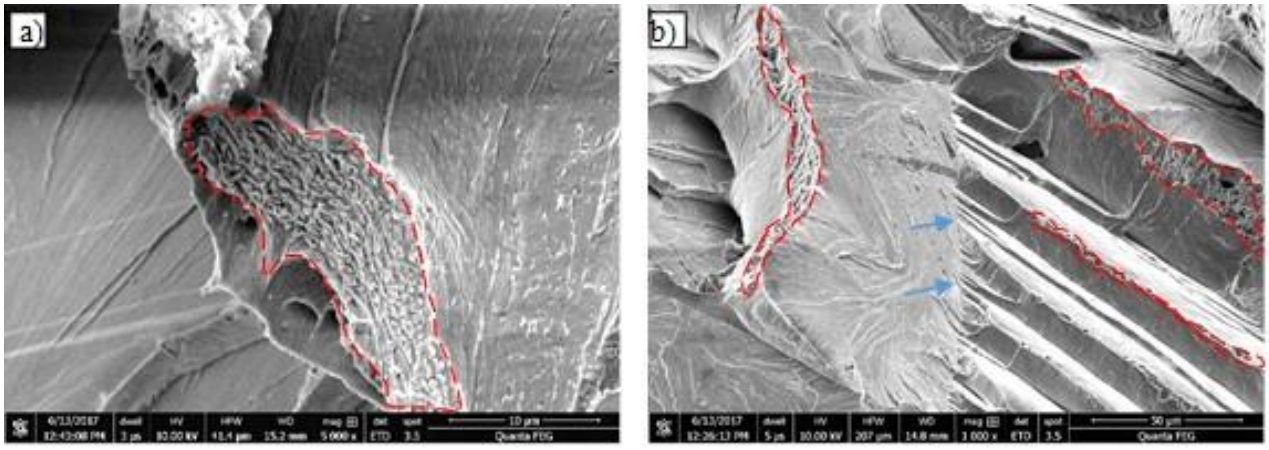

Fig. 10. Surface of the brittle fracture on 1.4742 steel grain boundary with chamfers on the edges

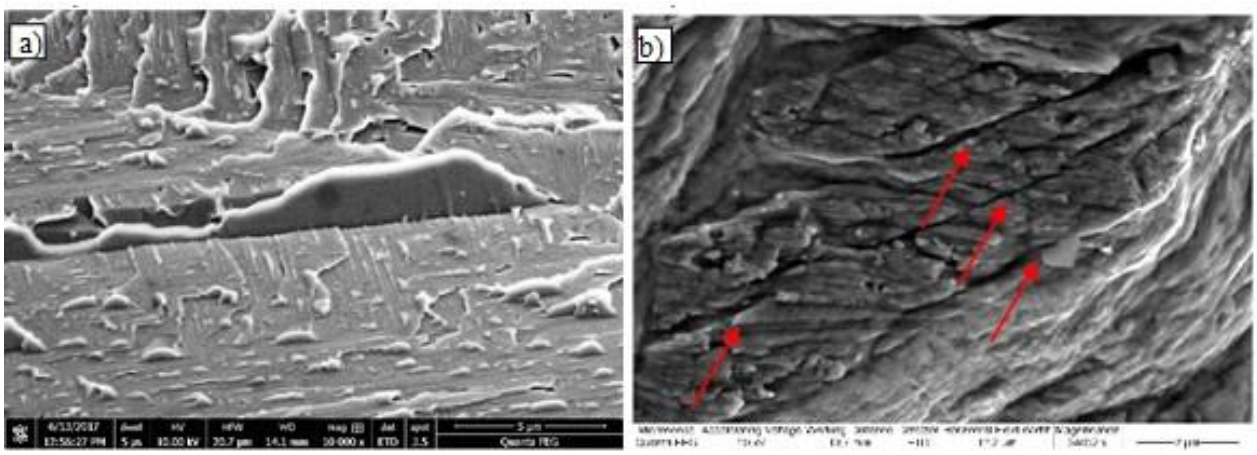

Fig. 11. Extrusions (a) and intrusions (b) obtained in a static tensile test

On the fractures, there were locally observed extrusions on the metal blades (Fig. 11 a) and intrusions (Fig. 11 b). In 1.4539 austenitic steel, there was observed a tendency to numerous intrusions, whereas in 1.4742 ferritic steel a tendency to extrusion was observed. It is related to a process of brittle and plastic fracturing.

CONCLUSIONS

The results for static tensile test fractures microfractography of welded joints of 1.4539 austenitic steel made with TIG method and made of 1.4742 ferritic steel with MAG method allow for formulation of the following conclusions:

- static tensile test fracture for the considered welded joint occurred outside the weld in the base material,
- joints made of 1.4539 austenitic steel were characterized with plastic fracturing, whereas, in the case of 1.4742 ferritic steel there was observed brittle fracturing mainly transcrystalline and partially on the grains boundaries,

- tensile strength limit was 547 MPa for 1.4742 steel and 589 MPa for 1.4539 steel. The difference in strength results, among others, from various fracturing mechanisms occurring in these joints.

LITERATURE

[1]. Kocańda S., Kocańda A., *Niskocyklowa wytrzymałość zmęczeniowa metali*, PWN, Warszawa, 1989.

[2]. Katarzyński S., Kocańda S., Zakrzwski M., *Badanie własności mechanicznych metali, Warszawa*, PWT, 1961.

[3]. Ramkumar K. D., Varma J. L. N., Chaitanya G., Choudhary A., Arivazhagan N., Narayanan S., *Effect of autogeneous GTA welding with and without flux addition on the microstructure and mechanical properties of AISI 904L joints*, Materials Science & Engineering A, vol. 636, pp. 1-9, 2015.

[4]. Balamurugan K., Abhilash A.P., Sathiya P., Naveen S. A., *Artificial neural network simulation and particle swarm optimisation of friction welding parameters of 904L superaustenitic stainless steel*, Multidiscipline Modeling in Materials and Structures, vol. 10 (2), pp. 250-264, 2014.

[5]. Sathiya P., Mishra M. ; Shanmugarajan B., *Effect of shielding gases on microstructure and mechanical properties of super austenitic stainless steel by hybrid welding*, Materials and Design, vol. 33, pp. 203-212, 2012.

[6]. Changjian G., Liu F., Tong W., Han Z., Chi Q., *Experimental Report on the Nano-identation Testing of Textured Stainless Steel 904 L and 316 L*, Procedia Engineering, Vol. 99, 2015, pp. 1268-1274, Procedia Engineering, vol. 99, pp.1268-1274, 2015.

[7]. Heino S., Knutson-Wedel E.M., Karlsson B., *Precipitation behaviour in heat affected zone of welded superaustenitic stainless steel*, Materials Science and Technology, vol.15(1), pp. 101-108, 1999.

[8]. Castro R., Cadenet J. J., *Metalurgia spawania stali odpornych na korozję i żarowytrzymałych,* WNT, Warszawa 1972, s. 22- 25, 111-112.

[9]. Ramkumar K. D., Chandrasekhar A., Srivastava A., Preyas H., Chandra S., Dev S., Arivazhagan N., *Effects of filler metals on the segregation, mechanical properties and hot corrosion behaviour of pulsed current gas tungsten arc welded super-austenitic stainless steel* Journal of Manufacturing Processes, vol. 24, pp.46-61, 2016.

[10]. Lu S., Wang X., Dong W., Li Y. *Effects of normalizing processes on microstructure and impact toughness in Ti-bearing weld metal of multilayer MAG welded HSLA steel*, ISIJ International, vol. 53(1), pp. 96-101, 2013.

[11]. Katarzyński S., Kocańda S., Zakrzewski M., *Badania własności mechanicznych metali*, WNT, 1967.